Full-waveform inversion and FWI imaging for land data

James Sheng, Cristina Reta-Tang*, Faqi Liu, TGS; Alfredo Vázquez Cantú, Alejandro Cabrales Vargas, Pemex

Summary

Velocity model building and imaging for land surveys are particularly challenging due to the complexities of the near surface model and strong noise.

In this abstract, we design a model building workflow for land seismic data that incorporates dynamic matching full-waveform inversion (DMFWI). DMFWI employs an objective function that uses multi-dimensional local cross correlations which minimize the impact of amplitudes and gives reliable results even in the presence of strong noise. We present the results of improved imaging for onshore surveys in Mexico.

We also explore full-waveform inversion (FWI) for imaging and utilize the high-resolution FWI velocity model to estimate reflectivity. The FWI images show enhanced features and provide an alternative image for poor S/N land datasets.

Introduction

FWI is a powerful tool for deriving velocity models widely used in the industry. There are many successful examples of its application for marine data, especially for surveys acquired with wide azimuths, long offsets and recorded low frequencies.

Building velocity models for land surveys is particularly challenging. Onshore seismic data is acquired on a non-flat datum (topography) which introduces elevation differences between the source and the receiver. In addition, the weathering layer, which is defined as a layer at or near the surface, possibly of heterogenous, unconsolidated material with low seismic velocities, can produce complex elastic waves. Recording of P waves on vertical component geophones also registers unwanted surface waves known as ground roll. Resolving the near surface velocity model is a crucial step in land imaging and traditionally addressed by refraction tomography and statics. Recently, FWI has been incorporated to update velocity models in complex geologies. Lemaistre, et al. (2018), combined first break picks with Laplace-Fourier FWI. Tang, et al. (2021) utilized a workflow that consisted of an alternated source and medium parameter(s) inversion. However, applying FWI to land data still presents challenges. Yilmaz, et al. (2022) extensively analyzed the use of FWI to update the near surface model. Using the vertical component of recoded seismic data, they argued that even elastic inversion, which should better describe land seismic data, is prone to inaccurate P-wave velocity-depth estimations of the near surface model due to complexities dealing with characteristics of the near surface (highly heterogeneous, strongly anisotropic, highly attenuating, etc.). As expected, attempting acoustic inversion to derive the P-velocity model of the near surface often fails because even if the data is limited to the early portion of the shot record, other types of waves (like converted waves) are generated in the near surface. According to Yilmaz, et al. (2022), only inverting early-arrival waveforms associated with first breaks or using first breaks for travel time tomography produced results robust enough to match well information. This is due in part to the greater control that can be exercised on first break picks, which can be edited or adjusted, while the amplitudes used for inversion are more prone to distortions if contaminated by noise or affected by the denoise algorithms.

Despite the challenges and limitations of the physical model (in our case acoustic), we attempt to include FWI in the model building workflow of two onshore surveys in Mexico.

To minimize the impact of the amplitudes, we use multi-channel dynamic matching full-waveform inversion (DMFWI) which promotes the kinematic difference in the inversion and provides more robust results even in the presence of noise (Mao, et al., 2020; Sheng, et al., 2020).

The model building workflow is designed to achieve geologically and data-consistent results for data acquired with limited offsets. The workflow includes the following steps:

a. Refraction tomography to build the near surface model. The near surface model is inserted into a smooth velocity model reaching maximum depth.
b. Long-wavelength tomographic updates to build a global model as accurate as possible below the near surface model to use as the initial model input to DMFWI.
c. DMFWI run from low to increasingly higher frequencies using early arrivals, including refractions and wide-angle reflections, to update the shallow portion of the model. This step targets the low to mid frequency components and has the most impact on migration kinematics.
d. Tomography to resolve the long wavelength of the mid to deep portion of the model. This step is optional, but often necessary due to the limited offsets of the surveys in our study areas and could be eliminated if the acquisition is more suitable for FWI.

Full-waveform inversion and FWI Imaging for land data

e.   Reflection DMFWI from low to increasingly higher frequencies with mainly reflection data to obtain fine details in the velocity model.

The workflow yields a high-resolution velocity model. Given the recent efforts to obtain an image or reflectivity based on extended FWI workflows (Zhang, et al., 2020; He, et al., 2021), we explore the usability on land data. A reflectivity image is derived as the normal derivative of the high-resolution velocity model obtained from high-frequency FWI. We find additional information on FWI images that is not evident on conventional migrations.

Methodology

First breaks are picked and used to derive the near surface model by refraction tomography. The near surface model is inserted to a smooth legacy sediment model. The first break picks are also useful for designing mutes, so that only early arrival, diving waves and wide-angle reflections are input to DMFWI. To precondition the data for DMFWI, minimal processing is applied including spike editing, ground roll noise attenuation and residual statics correction. The velocity model is calibrated to checkshot information and is updated by global reflection tomography. Anisotropy parameters are derived using focusing analysis (Cai, et al., 2009). The velocity and anisotropy models are the starting point for DMFWI.

We apply the DMFWI algorithm which maximizes multi-dimensional local crosscorrelations between synthetic and observed data. The window used in DMFWI is localized both in time and space which gives more reliable measurements of the correlations between input data and synthetic data, and allows more focus on kinematic information. The window size is frequency dependent which is naturally embedded in multi-scale FWI algorithms. The useful signal is promoted during inversion. Since the lateral information is used, the multi-channel algorithm can mitigate the influence of noise in the input data and make the inversion more robust overcoming the poor S/N ratio challenges typical of land acquisitions.

The FWI reflectivity image is calculated by a Snell's law-based approach directly from the high-resolution velocity model inverted from FWI (He, et al, 2021). The reflection coefficient at zero incident angle is proportional to the impedance contrast at the two sides of an interface.

Examples

The first case example includes several surveys acquired with dynamite and a limited number of shots acquired with vibroseis. The maximum offsets vary between 4494 m to 8209 m. Only 24 % of the study area is covered with offsets of 8209 m which imposes limitations to the penetration of diving waves in most areas. The noise in the data also limits the minimum usable frequency for FWI to 5 Hz. Minimum phase wavelets are obtained from data spectrum and used during FWI. We use a finite-difference method with low velocity and low density padding above topography to generate acoustic synthetic data, which due to the gentle topography of the study area, is adequate for our case. In this test, only dynamite acquisition is selected as input for DMFWI. The shots are muted to limit the energy to early arrivals, diving waves and wide-angle reflections. DMFWI is run with increasingly higher frequency bands, up to a maximum frequency of 15 Hz.

The starting model to DMFWI includes the near surface model from refraction tomography inserted into a smoothed version of the legacy models. The model is then updated with passes of global tomography. Figure 1a shows the starting model for DMFWI and Figure 1c shows the model after the DMFWI update. The complex faulting above the salt body, and the limited offsets to estimate curvatures in depth, contribute to unresolved tomographic velocity updates. The resolution of the tomographic velocity is insufficient to impact the image in the faulted area. Figures 1b and Figure 1d show Kirchhoff PSDM gathers before and after DMFWI velocity updates respectively. Clearly, the gathers are flatter after DMFWI. Figures 2a and 2b show Kirchhoff PSDM images migrated with the velocity models before and after FWI updates. The events above the salt body are more focused and the fault planes are better defined on the image migrated with the DMFWI updated model.

The velocity model building workflow continues with additional passes of multi-azimuth tomography to update the middle and deeper parts of the section and includes interpretation of the allochthonous salt bodies, carbonates, and autochthonous salt.

Finally, we run reflection DMFWI up to 25 Hz to obtain a high-resolution velocity model and generate FWI images by calculating the normal derivative of the FWI velocity model. This image benefits from the contribution of the full wavefield data (diving-wave, reflection energy) that is used in FWI to invert for velocity.

Figures 3a and 3b shows raw RTM images migrated at 20 Hz with the model before and after DMFWI update. The corresponding velocity models are overlaid. Figures 3c and 3d show a comparison between raw RTM and FWI image computed from the 25 Hz DMFWI velocity model. The FWI image has better defined events and faults (indicated with red arrows) due to the iterative least-squares data fitting, which enhances illumination and reduces artifacts.

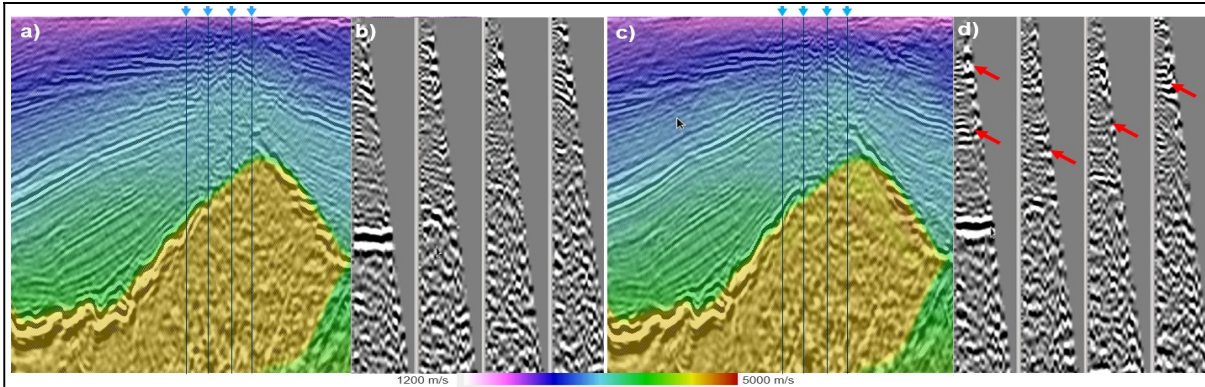# Full-waveform inversion and FWI Imaging for land data

Figure 1: a) Initial model overlaid on Kirchhoff stack; b) gathers migrated with initial model; c) model after DMFWI overlaid on Kirchhoff stack; d) gathers migrated with model after DMFWI. Blue arrows indicate gather locations. Red arrows indicate better flattening of the gathers.

Nevertheless, some events may not be real, due to the limitations of the acoustic physical model. We also observe that areas with acquisition gaps tend to get filled in.

The second dataset is the merge of several surveys acquired with mainly dynamite and a reduced number of shots with vibroseis. The maximum offsets vary between 5318 m to 6550 m. The main area of interest is covered by a survey with approximately 5496 m of maximum offset.

The sedimentary model at the target level consists of platform carbonate rocks. The study area presents a structural high generated by the evacuation of salt. The potential targets are dipping carbonates a few hundred meters in thickness located below Tertiary salt. The allochthonous salt extends upwards and cuts the beds of interest.

The velocity model is built according to the workflow previously described. The results after reflection DMFWI

are displayed in Figure 4. Figures 4a and 4c show conventional 20 Hz RTMs migrated with velocity models from before and after DMFWI updates. The RTM after FWI update shows better definition of the carbonate layer, and a thrust becomes clearer. The events below the carbonate are also more continuous. Areas of improvements are marked with green arrows. Figure 4e is the FWI image obtained from the high resolution DMFWI velocity model at 30 Hz. Additional enhancements are observed and indicated with blue arrows. Figures 4b and 4d show RTMs with the corresponding model overlaid. Figure 4f shows the FWI image overlaying the model obtained from DMFWI.

Conclusions

Despite the challenges of land data and limitations of the acquisition parameters of the surveys in the study areas discussed in this paper, we successfully incorporate DMFWI into a robust model building workflow for land
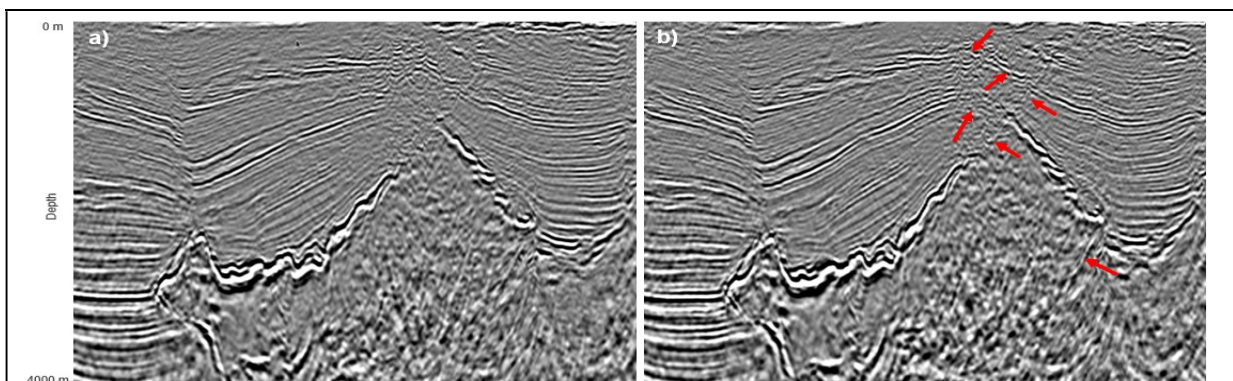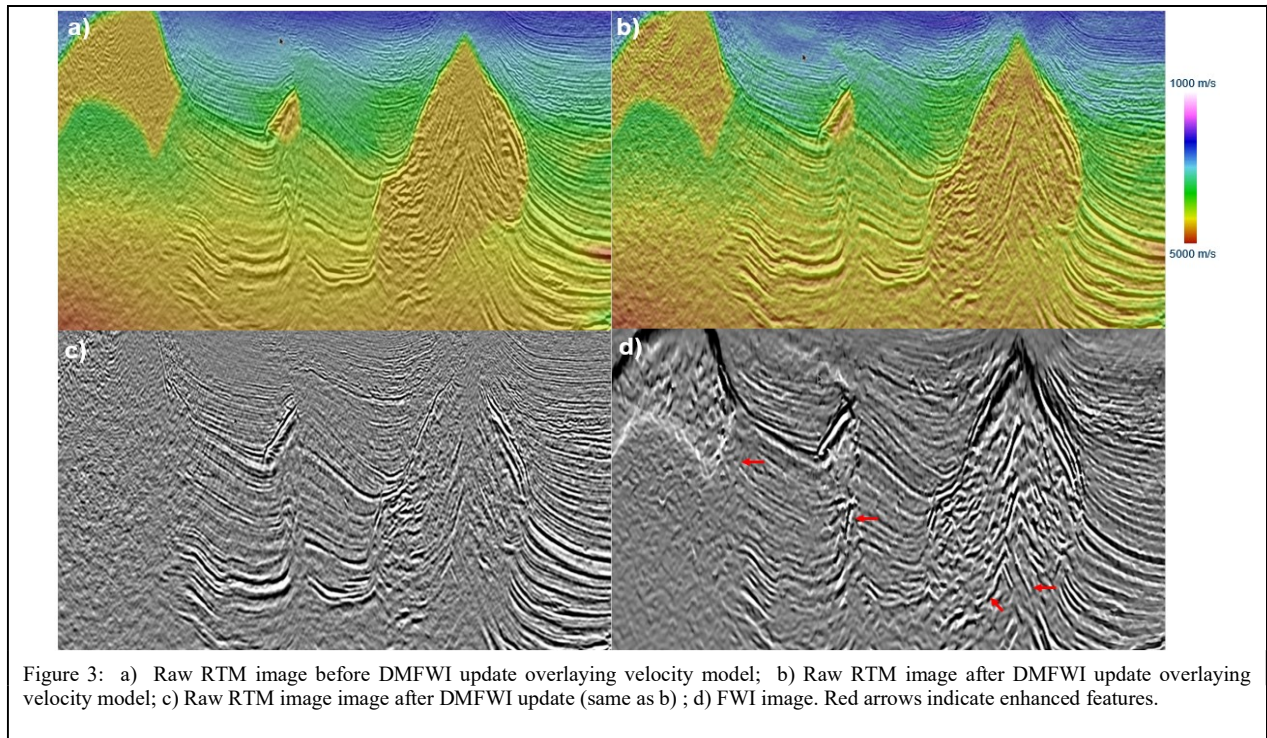

Figure 2: a) Kirchhoff PSDM before PSDM before DMFWI velocity update; b) Kirchhoff PSDM after DMFWI velocity update. Red arrows indicate areas with better focusing.

Full-waveform inversion and FWI Imaging for land data

Figure 3: a) Raw RTM image before DMFWI update overlaying velocity model; b) Raw RTM image after DMFWI update overlaying velocity model; c) Raw RTM image image after DMFWI update (same as b) ; d) FWI image. Red arrows indicate enhanced features.

data yielding a high-resolution velocity model. We explore the application of an extended FWI workflow to generate a reflectivity image that is estimated as the normal derivative of the high-resolution FWI model obtained from reflection DMFWI. The FWI images exhibit enhanced events which have benefited from the iterative time domain least-squares data fitting involved. Inverting the FWI velocity model to reflectivity images show potential for improved interpretability of poorly illuminated and low S/N ratio land datasets.

Figure 4: a) RTM before FWI; b) Starting model for reflection DMFWI overlaying corresponding RTM c) RTM after DMFWI; d) Model after reflection DMFWI overlaying corresponding RTM; e) FWI image; f) Model after reflection DMFWI overlaying FWI image. Green and blue arrows indicate enhanced features when comparing to areas indicated with red arrows on 4a)